Available online at www.sciencedirect.com
SCIENCE DIRECT
Catalysis Today 105 (2005) 618–622
CATALYSIS TODAY
www.elsevier.com/locate/cattod

Tuning of nanostructured SBA-15 silica using phosphoric acid

Raghuraman Pitchumani, Wenjiang Li, Marc-Olivier Coppens *

Physical Chemistry and Molecular Thermodynamics, DelftChemTech, TU Delft, Julianalaan 136, 2628 BL Delft, The Netherlands

Available online 11 July 2005

Abstract

A simple method is described to synthesize mesoporous SBA-15 with controlled distinct morphologies. Using the same initial synthesis mixture composition consisting of non-ionic P123 block co-polymer, tetra-ethyl orthosilicate as silica source and phosphoric acid, well-ordered mesoporous films, cakes, fibers and bundle-like structures were produced simply by changing the stirring rate. Free-standing films at the air–water interface and cake-like structures were obtained simultaneously under static conditions. On the other hand, fibers and bundles of threads resulted under vigorous and slow stirring conditions, respectively. Transmission electron microscopy (TEM) images of these bundles revealed straight parallel nanochannels oriented along the long axis of the bundles. X-ray fluorescence (XRF) measurements of the calcined samples indicated the presence of phosphorus, which might provide additional Brønsted acid sites for potential applications in catalysis.

Keywords: Mesoporous; Hexagonal; SBA-15

1. Introduction

SBA-15 is a mesoporous SiO_2 with a hexagonal arrangement of channels with diameters in the range of 2–30 nm [1]. Its advantages include high thermal stability and relatively thick silica walls with a network of micropores in the walls in addition to well-ordered mesopores. SBA-15 is synthesized using a non-ionic surfactant P123 (block co-polymer EO_{20}–PO_{70}–EO_{20}, where EO is ethylene oxide and PO is propylene oxide) in the presence of strong acids like HCl.

Since the pioneering work reported by researchers at Mobil [2], such surfactant templated mesoporous materials have found several applications in catalysis, gas sensing, separation and optics [3]. The synthesis process of mesoporous materials like SBA-15 involves the formation of organic–inorganic composites by a self-assembly process, where the organic phase is organized on a mesocopic scale and serves as a template for the inorganic component. Different mesostructures and pore sizes can be obtained by adjusting the synthesis conditions and nature of the surfactant. Mesoporous materials in the form of films [4], monoliths [5], spheres [6], rod-like structures [7], fibers [8] and crystals [9] have been obtained in block co-polymer templating systems. Mesoporous films have been grown at air–water and mica–water interfaces through an interfacial silica-surfactant self-assembly process [10,11]. Zhao et al. [12] reported the formation of continuous mesoporous silica films with large periodic cage and pore structures using poly-(ethylene oxide) non-ionic surfactants as structure directing agents in a dip-coating process. The films exhibited high thermal stability upon calcination at 450 °C and were crack free for a thickness less than 1 μm. The thickness of the film was varied uniformly by adjusting the dip-coating rate or the coating solution concentration. These mesostructured films might find use, in addition to catalysis, as membranes for biomolecular separations, sensors, ordered ceramic matrix composites and mesostructured composites [10]. Highly ordered mesoporous SBA-15 fibers over 100 μm in length with a uniform diameter were grown using tetra-methyl orthosilicate (TMOS) under acidic conditions [6]. Ordered and optically transparent mesoporous silica fibers were synthesized in a two-phase system at room temperature and have been demonstrated to have potential as high-surface area optical waveguides [13]. Yang

* Corresponding author. Tel.: +31 15 278 4399; fax: +31 15 278 8047.
E-mail address: M.O.Coppens@tnw.tudelft.nl (M.-O. Coppens).

0920-5861/$ – see front matter
doi:10.1016/j.cattod.2005.06.002

et al. [8] employed a simple process for making mesoporous fibers with large and accessible pores. These fibers were uniaxially aligned and possessed either 3D hexagonal cage or 2D hexagonal channel structures.

In the present study, we utilize a simple approach to selectively synthesize unique morphologies of SBA-15 from a mixture that is similar to the one conventionally used [1], except that it includes a weak acid H_3PO_4 instead of the strong acid HCl. By simply controlling the stirring rate, shapes of a broader variety than when using HCl are obtained from an identical starting mixture.

2. Experimental

2.1. Material synthesis

A sol–gel process was employed to produce the materials. Different samples were prepared from the same initial aqueous solution. 3.0 g of Pluronic P123 were dissolved in 5.0 g of phosphoric acid (85 wt%) and 60 ml of deionized water at 40 °C to obtain a clear solution. 8.0 ml of tetra-ethyl orthosilicate (TEOS) was quickly added to this mixture, while stirring at 40 °C with a magnetic stirrer. Excess water was added to make up the solution to 80 ml. The molar composition of the starting solution was TEOS:P123:H_3PO_4:H_2O = 1.0:0.015:1.23:111.1.

Three sets of experiments were performed. In the first set, stirring (at 500 rpm) was stopped 2 min after the addition of TEOS and the mixture was subsequently kept under static conditions at 40 °C for 48 h. In the second and third set of experiments the solution was stirred, either vigorously (423 rpm) or slowly (134 rpm) at 40 °C for 24 h. The solid products obtained from the three batches were transferred to autoclaves and aged at 100 °C for 24 h. The resulting products were recovered by filtration, washed with deionized water, and dried in an oven at 80 °C. To remove the organic template, the samples were calcined at 250 °C for 3 h and then at 550 °C for 7 h using a heating rate of 5 °C/min.

2.2. Material characterization

Powder X-ray diffraction (XRD) patterns of products obtained from the first set of experiments were recorded using a Bruker-AXS D5005 diffractometer with a Co Kα X-ray source (λ_{Co} = 0.179026 nm). XRD patterns of products produced from the other sets were recorded using a Bruker-AXS D8 Advance X-ray diffractometer equipped with a Vantec position sensitive detector using Co Kα radiation (λ_{Co} = 0.179026 nm). Scanning electron microscopy (SEM) images of products from the first set of experiments were obtained with a Philips XL-20 SEM and of the other sets with a JEOL JSM-6500F microscope. Transmission electron micrographs (TEM) were recorded using a Philips CM30T electron microscope with a LaB_6 filament as the electron source, operated at 300 kV. Samples were mounted on a microgrid carbon polymer, which was fixed on a copper grid. A specimen of the film was prepared by an ultrathin microtoming method, in which the film sample was embedded in an epoxy resin; thin slices were cut parallel to the film surface and then placed on the grid.

Nitrogen adsorption–desorption isotherms were measured using a Quantachrome Autosorb-6B sorption analyzer. Prior to the isotherm measurements, the samples were degassed at 350 °C overnight.

The phosphorus content in the calcined samples was determined from X-ray fluorescence (XRF) measurements done on a Philips PW1480 spectrometer. The concentrations were calculated with the semi quantitative program UniQuant5®.

3. Results and discussion

Fig. 1 shows SEM images of the materials synthesized under static conditions. Initially, freestanding, transparent films were produced at the air–water interface.

Subsequent ageing and calcination resulted in a film with a smooth, crack free continuous surface having a uniform thickness of 40 μm (as seen in Fig. 2a). It was also observed

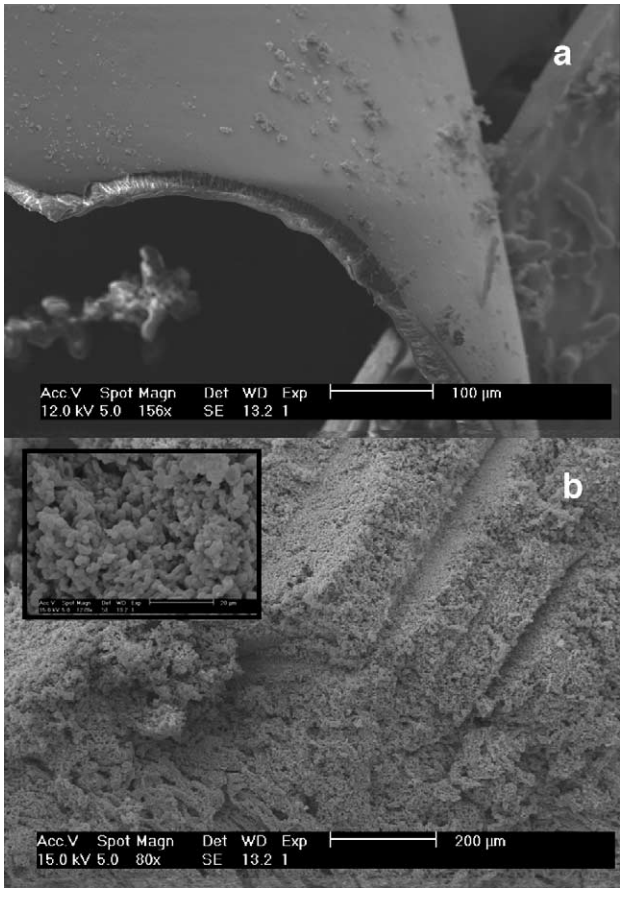

Fig. 1. SEM of calcined (a) film and (b) cake.

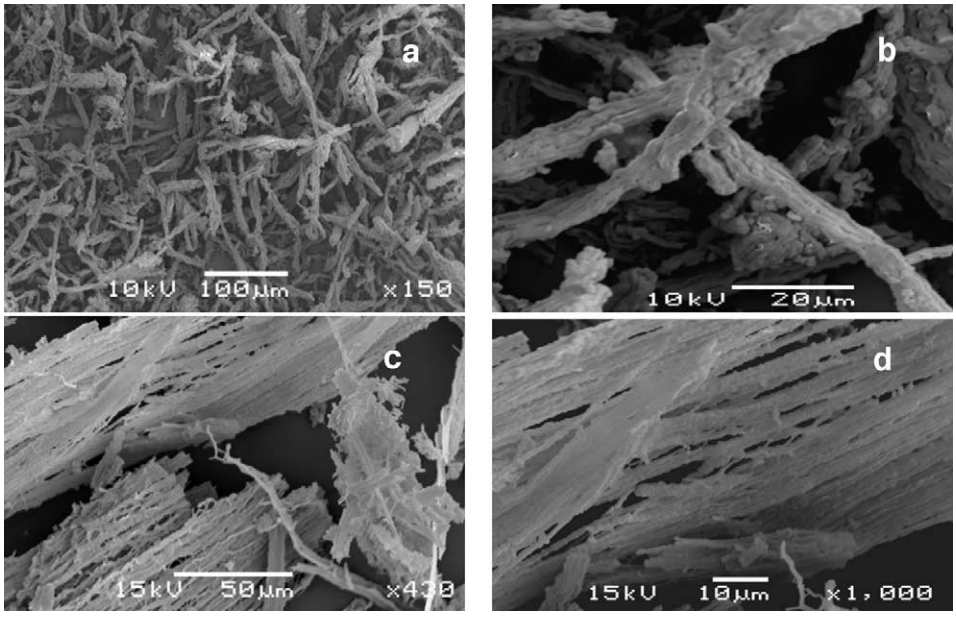

Fig. 2. SEM images of SBA-15 fibers (a and b) and bundles (c and d).

that thin rods extended from the surface of the film and into the solution. On reaching a certain length, these rods got detached from the film surface.

A white precipitate was formed as well. Calcination of the aged sample resulted in a cake-like structure as shown in Fig. 1b. Close observation of the cake indicated that it was composed of a closely packed network of particulate grains (inset of Fig. 1b). The void existing between these grains (inter-particle space) provides macroporosity (in addition to the mesoporosity) resulting in a hierarchical porous material.

Materials prepared under vigorous stirring conditions resulted in fiber-like morphologies. Fig. 2(a and b) show SEM images of fibers extending over 100 μm in length and with a width of 10 μm. Close examination of these fibers indicated that the fibers were made up of several individual segments coupled together along their length (Fig. 2b).

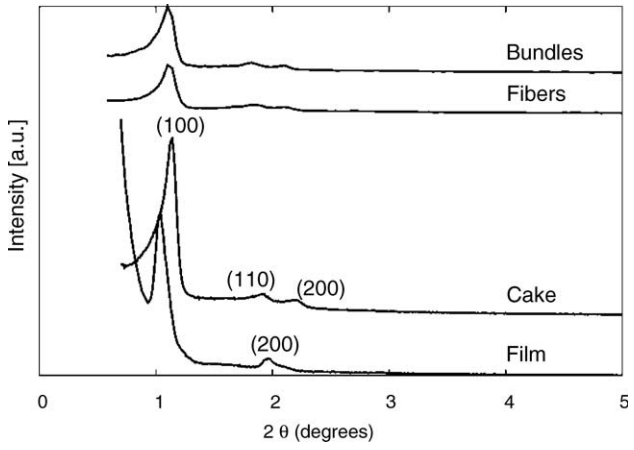

Fig. 3. X-ray diffraction patterns of different samples.

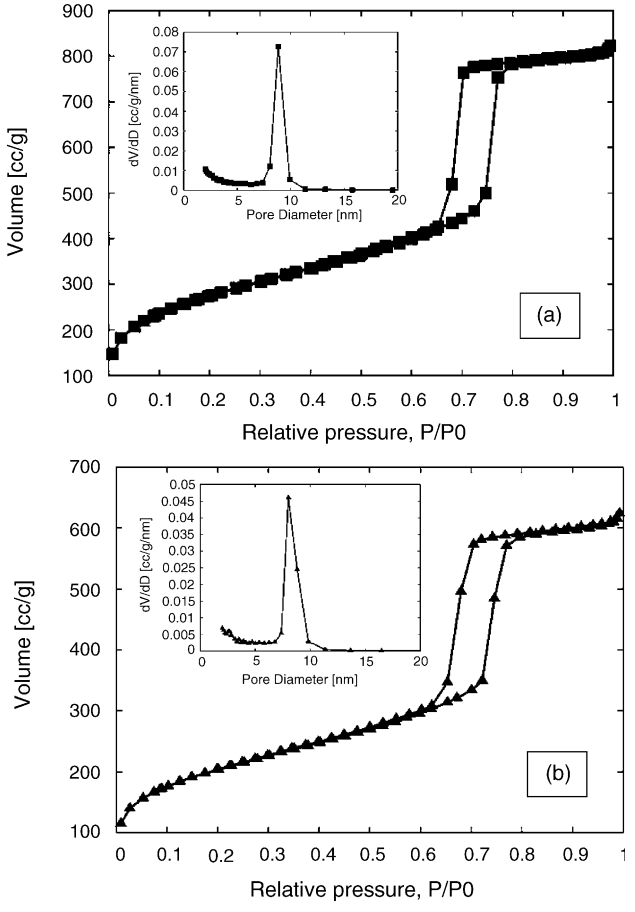

Fig. 4. N_2 adsorption–desorption isotherms and (inset) pore size distributions of (a) fibers and (b) bundles calculated using the BJH model from the adsorption branch of the isotherms.

Products synthesized under slow stirring conditions had a unique morphology in the form of bundles as shown in Fig. 2(c and d), several 100 μm in length and with a width of at least 50 μm. The bundles are composed of long thin thread-like structures fused together (Fig. 2d).

Fig. 3 shows the X-ray diffraction patterns of the different morphologies obtained by changing the stirring rate. The XRD patterns of fibers, bundles and cakes show sharp peaks corresponding to (1 0 0), (1 1 0) and (2 0 0) reflections indicating highly ordered mesoporous SBA-15 with a 2D hexagonal symmetry (*p6mm*) [14]. In comparison, the absence of the (1 1 0) reflection for the film suggests that the pore channels are aligned parallel to the film surface. Similar observations have been made by Zhao et al. [12] who synthesized mesoporous SBA-15 films on polished silicon wafers and confirmed the orientation of the pore channels from TEM images. The cell parameter of films, cakes, fibers and bundles (calculated using the formula $a = 2d_{100}/\sqrt{3}$, d_{100} is the interplanar spacing) is 11.4, 10.4, 10.6 and 10.6 nm, respectively.

The calcined film has a Brunauer–Emmett–Teller (BET) surface area of 833 m^2/g, a pore volume of 0.88 cm^3/g and an average pore size of 8.0 nm calculated by using the Barrett–Joyner–Halenda (BJH) model applied to the adsorption branch of the isotherm. The calcined cake has a BET surface area of 827 m^2/g, a pore volume of 1.04 cm^3/g and a BJH pore size of around 8.0 nm.

The N_2 adsorption–desorption isotherms (Fig. 4) of calcined silica fibers and bundles are type IV with a clear type H_1 hysteresis loop. The isotherms and corresponding pore size distributions (inset of Fig. 4a and b) indicate the presence of a narrow pore size distribution in both fibers and bundles. The fibers have a BJH pore size of 8.0 nm (calculated from the adsorption isotherm), a BET surface area of 626 m^2/g and a pore volume of 0.83 cm^3/g. The bundles have a slightly larger pore size of 8.8 nm, a much higher BET surface area of 968 m^2/g and a pore volume of 1.3 cm^3/g.

Insight into the pore structure of the mesoporous silica bundles is revealed by TEM (Fig. 5). Well-ordered

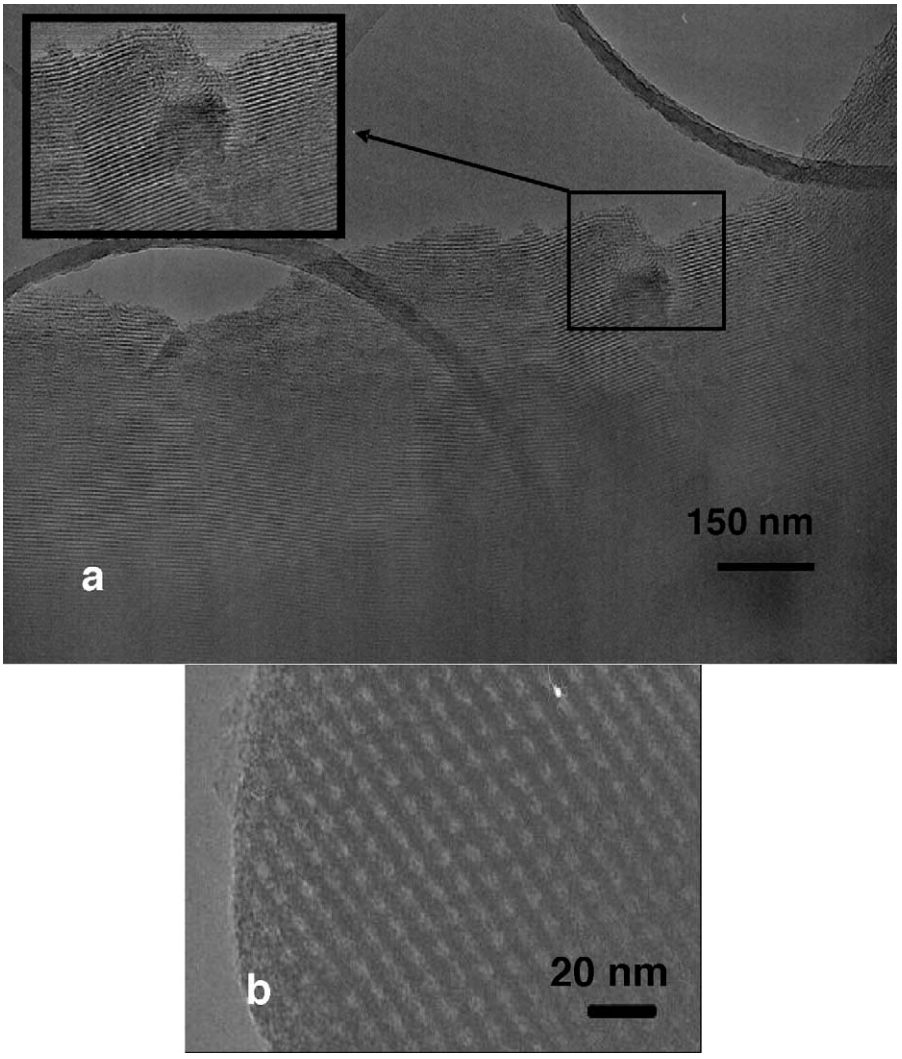

Fig. 5. TEM images of calcined silica bundles along directions (a) [1 1 0] and (b) [1 0 0].

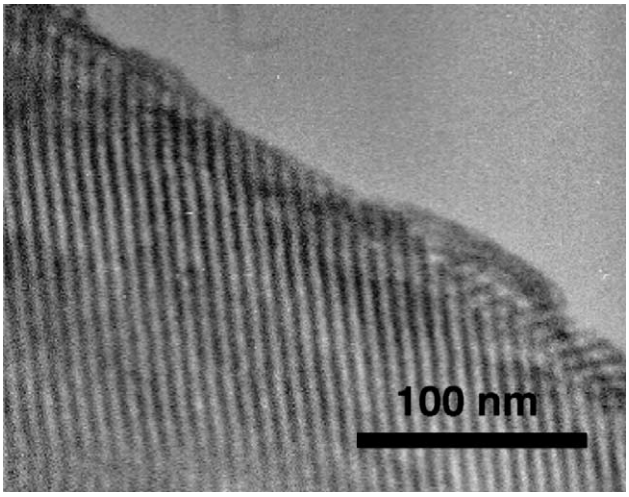

Fig. 6. TEM image of mesoporous SBA-15 film (topview).

Table 1
XRF measurements of fibers and bundles

Sample	Si/P (mol/mol)	
	Initial gel (calculated)	Calcined (XRF measurements)
Fibers	0.81	190.1
Bundles	0.81	18.0

hexagonal arrays of pores were found in the bundle cross-section (Fig. 5b). Fig. 5a shows the high structural order, with parallel nanochannels of a uniform diameter that follow the long axis of the bundles with high fidelity. A TEM image of the top view of the microtomed film (Fig. 6) shows that the channels run predominantly parallel to the film surface. This is in agreement with the observed XRD pattern (Fig. 3).

The stirring rate can thus be used effectively to tune the morphology of SBA-15. The different shear rate associated with different stirring conditions influences the shape and aggregation of micelles, as well as the interfacial growth of the silica-surfactant mesophase, resulting in distinct morphologies. Note again that the starting composition was identical in all experiments. It is not clear yet how the H_3PO_4 affects the morphology.

X-ray fluorescence measurements of the fibers and bundles indicated the presence of phosphorus in the silica framework even after calcination at 550 °C (Table 1). The phosphorus content in the fibers was more than 10 times that present in the bundles. The generation of Brønsted acidity is proposed due to interaction of the H_3PO_4 with the silica species during hydrolysis to form P–O–Si bonds. Although the hydroxyl groups of phosphoric acid can be removed by dehydration during high temperature calcination, the hydroxyl groups can also be restored after adsorption of moisture from the air. These restored hydroxyl groups on phosphorus have the ability to donate protons, producing mainly Brønsted acid sites on the surface of SBA-15. This improves the overall acidity of SBA-15 and could be used as a promising selective catalyst for specific reactions that need only Brønsted acidity, for instance dehydration of isopropanol [15]. Phosphorus containing catalysts have been shown to improve the activity for selective oxidation of hydrocarbons [16] and improve hydrothermal stability of the mesoporous framework [17].

4. Conclusions

In summary, we successfully synthesized distinct morphologies (films, cakes, fibers and bundles) of highly ordered mesoporous SBA-15 in the presence of weak acid (H_3PO_4) by simply changing the stirring rate. XRF measurements indicated the presence of phosphorus in the silica framework generating additional Brønsted acid sites. TEM images of the bundles revealed parallel nanochannels oriented along the long axis of the bundles.

Acknowledgements

We thank Albemarle Catalysts, the Dutch National Science Foundation (NWO, via a CW/PIONIER grant) and Delft University of Technology for their financial support. We also acknowledge Mr. J.C. Groen, Mr. S. Brouwer for N_2 adsorption measurements, Mr. N. van der Pers for the XRD measurements, Mr. J. Padmos for the XRF measurements and Dr. P.J. Kooyman and Dr. C. Peet for the TEM images.

References

[1] D. Zhao, Q. Huo, J. Feng, B.F. Chmelka, G.D. Stucky, J. Am. Chem. Soc. 120 (1998) 6024.
[2] C.T. Kresge, M.E. Leonowicz, W.J. Roth, J.C. Vartuli, J.S. Beck, Nature 359 (1992) 710.
[3] P. Selvam, S.K. Bhatia, C.G. Sonwane, Ind. Eng. Chem. Res. 40 (2001) 3237.
[4] H. Miyata, T. Nama, M. Watanabe, K. Kuroda, Chem. Mater. 14 (2002) 766.
[5] H.F. Yang, Q.H. Shi, B.Z. Tian, S.H. Xie, F.Q. Zang, Y. Yan, B. Tu, D.Y. Zhao, Chem. Mater. 15 (2003) 536.
[6] D. Zhao, J. Sun, A. Li, G.D. Stucky, Chem. Mater. 12 (2000) 275.
[7] P. Schmidt-Winkel, P.D. Yang, D.I. Margolese, B.F. Chmelka, G.D. Stucky, Adv. Mater. 11 (1999) 303.
[8] P.D. Yang, D.Y. Zhao, B.F. Chmelka, G.D. Stucky, Chem. Mater. 11 (1998) 2033.
[9] C.Z. Yu, B.Z. Tian, J. Fan, G.D. Stucky, D.Y. Zhao, J. Am. Chem. Soc. 124 (2002) 4556.
[10] H. Yang, N. Coombs, I. Sokolov, G.A. Ozin, Nature 381 (1996) 589.
[11] H. Yang, A. Kuperman, N. Coombs, S.M. Afara, G.A. Ozin, Nature 379 (1996) 703.
[12] D. Zhao, P. Yang, N. Melosh, J. Feng, B.F. Chmelka, G.D. Stucky, Adv. Mater. 10 (1998) 1380.
[13] Q. Huo, D. Zhao, J. Feng, K. Weston, S.K. Buratto, G.D. Stucky, S. Schacht, F. Schüth, Adv. Mater. 9 (1997) 974.
[14] D.Y. Zhao, J.L. Feng, Q.S. Huo, N. Melosh, G.H. Fredrickson, B.F. Chmelka, G.D. Stucky, Science 279 (1998) 548.
[15] S. Kawi, S.C. Chen, P.L. Chew, J. Mater. Chem. 12 (2002) 1582.
[16] L. Hagey, H. de Lasa, Chem. Eng. Sci. 54 (1999) 3391.
[17] L.M. Huang, Q.Z. Li, Stud. Surf. Sci. Cat. 129 (2000) 93.